The Physics of Space Plasmas

Magnetic Storms, Substorms and the Generalized Ohm's Law

William J. Burke

27 November 2012

University of Massachusetts, Lowell

BOSTON COLLEGE
ISR
INSTITUTE FOR SCIENTIFIC RESEARCH

Lecture 10

- **Geomagnetic Storms: (continued)**
  - **Large amplitude FACs and ionospheric conductance sources**
  - **The transmission-line analogy**

- **Geomagnetic Substorms:**
  - **Growth-phase phenomenology near geostationary altitude**
  - **NEXL versus SCW pictures: a perennial controversy**

- **Applications of the Generalized Ohm's Law: CLUSTER**

- $\nabla p = \mathbf{j} \times \mathbf{B}$ **=> Ingredients of** $j_{||}$

Magnetic Storms, Substorms & Generalized Ohm's Law

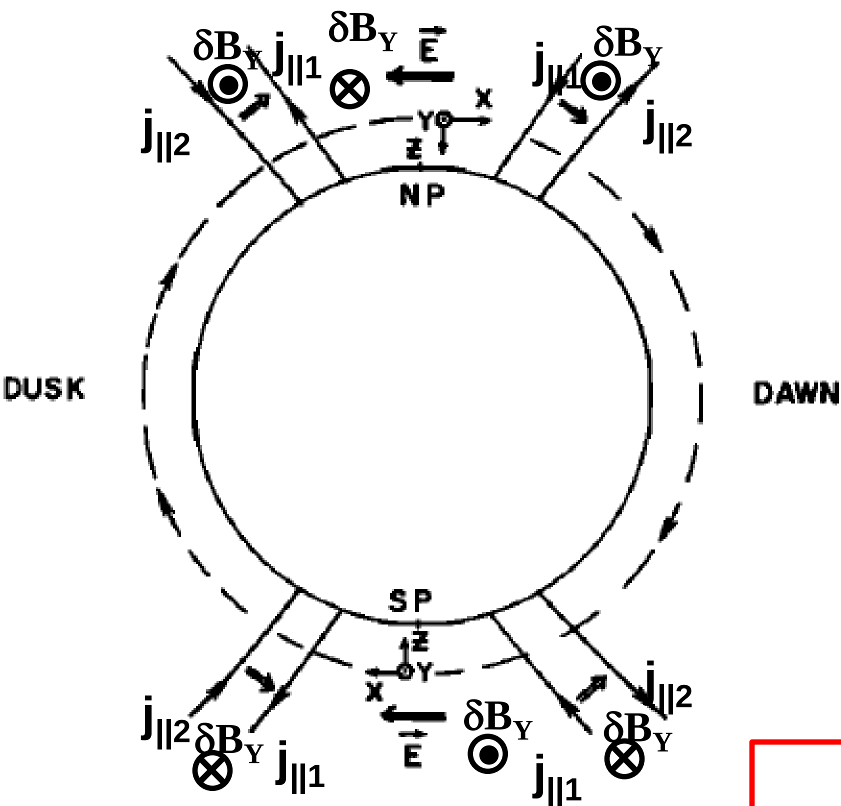

$$\nabla \times \mathbf{E} = 0$$

$$\nabla \cdot \mathbf{E} = \rho_e / \varepsilon_0$$

$$(\nabla \times \delta\mathbf{B})_{\|} = \mu_0 j_{\|}$$

$$\nabla \cdot \delta\mathbf{B} = 0$$

$$\frac{\partial j_{\|}}{\partial s} = -\nabla \cdot I_{\perp}$$

$$\mathbf{I}_{\perp} = \sigma_P \mathbf{E} - \sigma_H \mathbf{E} \times \hat{\mathbf{b}}$$

$$j_{\|} = \nabla \cdot \left[\Sigma_P \mathbf{E} - \Sigma_H \mathbf{E} \times \hat{\mathbf{b}} \right] = \nabla \cdot \Sigma_P \mathbf{E} - \mathbf{E} \times \hat{\mathbf{b}} \cdot \nabla \Sigma_H$$

$$(\nabla \times \delta\mathbf{B})_{\|} = \mu_0 \left[\nabla \cdot \Sigma_P \mathbf{E} - \mathbf{E} \times \hat{\mathbf{b}} \cdot \nabla \Sigma_H \right]$$

(A) **Normal Incidence**

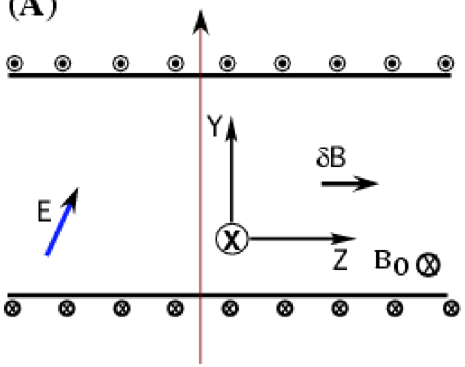

(B) **Oblique Incidence**

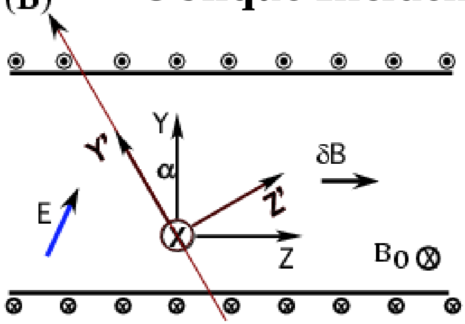

If $(\alpha = 0)$, then $\nabla_\perp \rightarrow \partial_Y$

$$j_\| = (1/\mu_0)\,[\partial_Y \delta B_Z] = (1/V_{sat}\,\mu_0)\,[\partial_t\, \delta B_Z]$$

$V_{sat} \approx 7.5$ km/s ➔ $1\ \mu A/m^2 \approx 9.4$ nT/s

$$J_\| = \int j_\|\, dY \;➔\; J_\| = (1/\mu_0)\,[\Delta\, \delta B_Z]$$

1 A/m ➔ $\Delta\, \delta B_Z = 1256$ nT

In **DMSP-centered coordinates:**

$$j_\| = \partial_Y [\Sigma_P E_Y - \Sigma_H E_Z] = (1/\mu_0)\,[\partial_Y \delta B_Z]$$

$$\partial_Y [\delta B_Z - \mu_0 (\Sigma_P E_Y - \Sigma_H E_Z)] = 0$$

Where δB_Z and E_Y vary in the same way

$$\Sigma_P \approx (1/\mu_0)\,[\Delta\, \delta B_Z / \Delta E_Y]$$

$$\mathbf{\Sigma_P (mho) \approx \Delta\, \delta B_Z (nT) / 1.256\, \Delta E_Y (mV/m)}$$

Magnetic Storms, Substorms & Generalized Ohm's Law

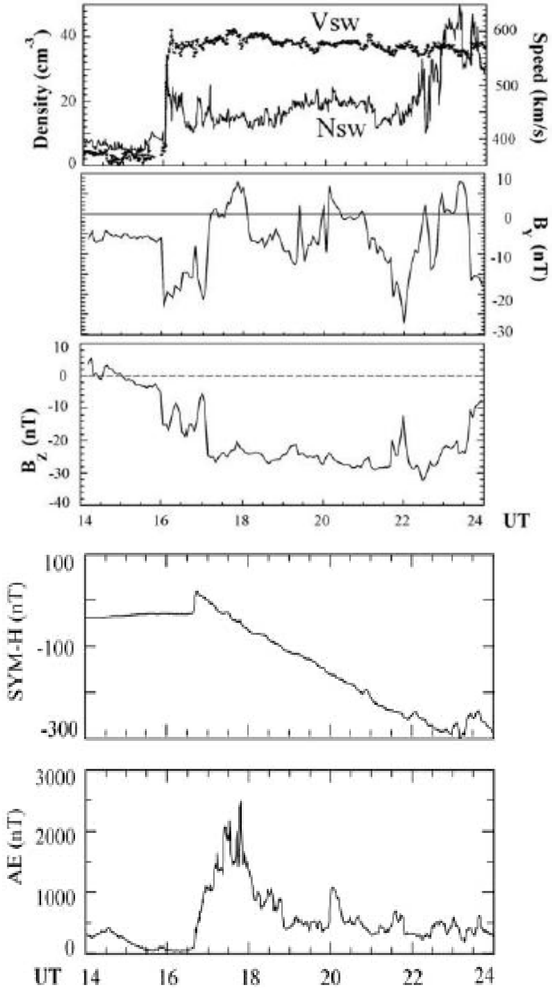

During the autumn of 2003 Cheryl Huang and I were studying the distribution and intensities of Region 1 and Region 2 FACs in support of an AFRL effort to model (empirically) the distributions of electric potentials in the global ionosphere.

The magnetic storm of 6 April 2000 radically changed our perceptions of stormtime M-I-T coupling and the directions of our future research.

Huang, C. Y. and W. J. Burke (2004) Transient sheets of field-aligned currents observed by DMSP during the main phase of a magnetic superstorm, *JGR, 109*, A06303.

Magnetic Storms, Substorms & Generalized Ohm's Law

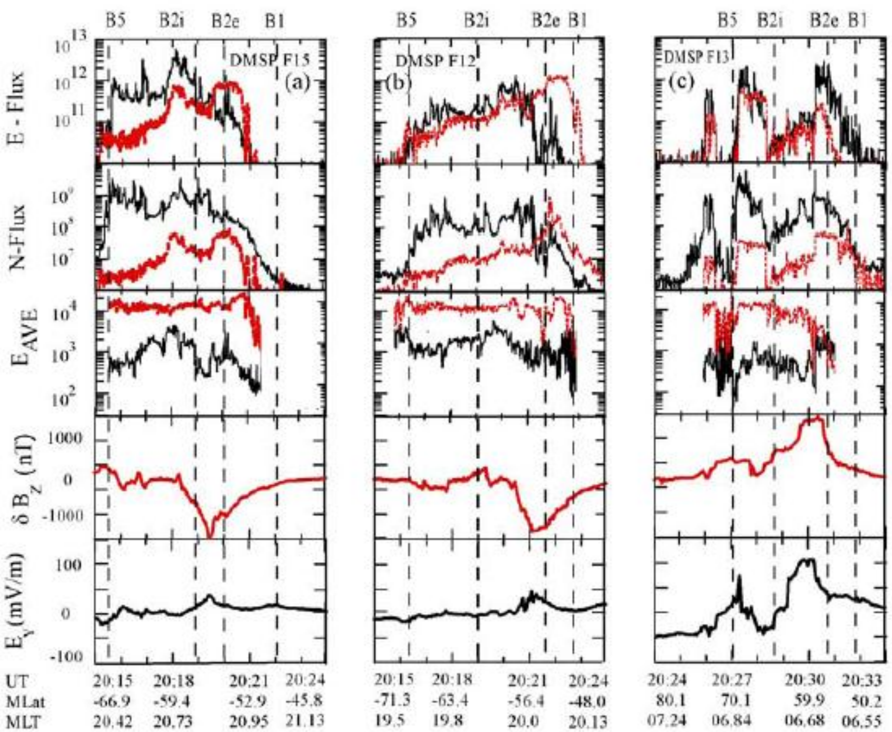

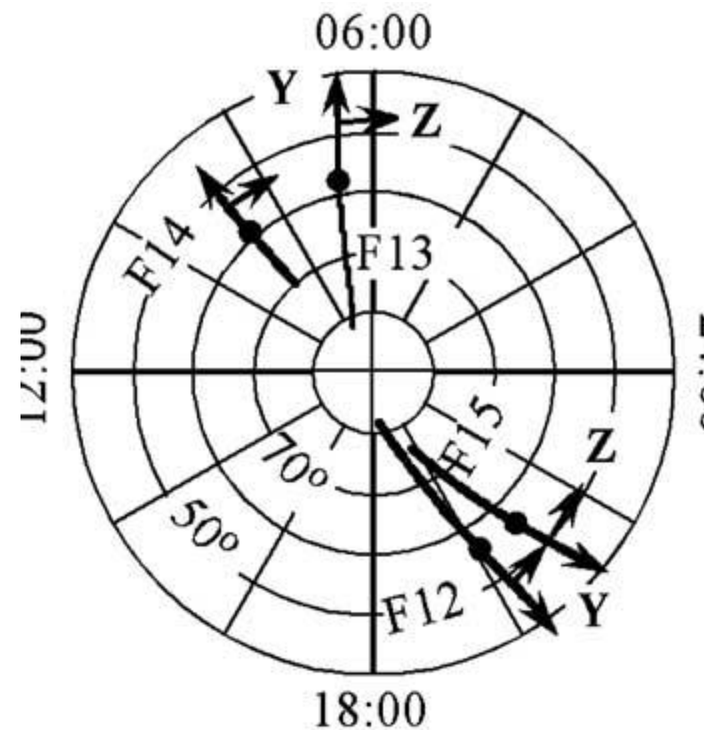

B5 => poleward boundary of auroral oval

B2i => ion isotropy boundary: stretched to quasi dipolar field

B2e => entry to main plasma sheet: e- energies no loner increase with latitude

B1 => equatorward boundary of auroral precipitation.

Magnetic Storms, Substorms & Generalized Ohm's Law

Table 1. Extrema of δB_Z and E_Y

DMSP	UT	MLAT	MLT	MLONG	GLAT	GLONG	$\lvert\delta B_Z\rvert$, nT	$\lvert E_Y\rvert$, mV/m
F12	2012.2	56.0°	19.9	66°	55.0°	14.5°	1326	41.5
F13	2030.3	58.7°	6.7	225°	63.0°	159.9°	1424	91.5
F14	2030.7	59.0°	8.4	255°	61.2°	199.8°	1354	82.9
F15	2019.4	55.9°	20.9	79°	52.1°	26.4°	1506	42.5

$$\Sigma_P\,(\mathrm{mho}) \approx \Delta\,\delta\,B_Z\,(\mathrm{nT}) / 1.256\,\Delta\,E_Y\,(\mathrm{mV/m}) \approx 25\ \mathrm{mho}$$

However, the much used equation for Pederson conductance derived from Chatanika ISR

$$\Sigma_P \quad [40\,E_{ave}\,\sqrt{(\Phi_E)}]\,/\,[16 + E_{ave}^2]$$

where E_{ave} is in keV and Φ_E is in ergs/cm^2-s , yield a Pederson conductance of about 5 mho.

Something was amiss. But what?

Magnetic Storms, Substorms & Generalized Ohm’s Law

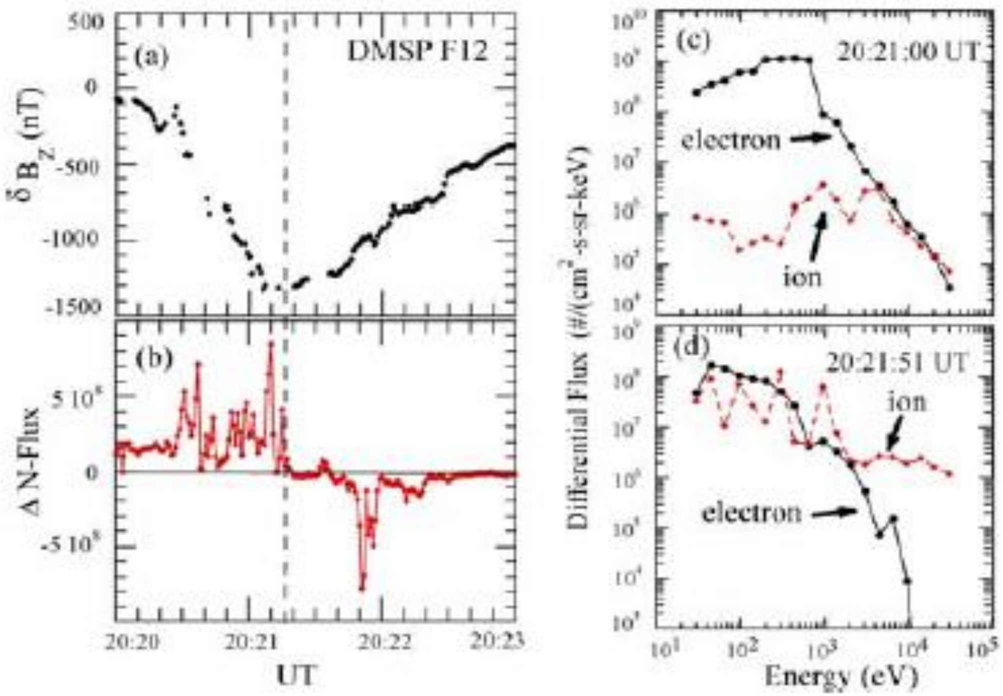

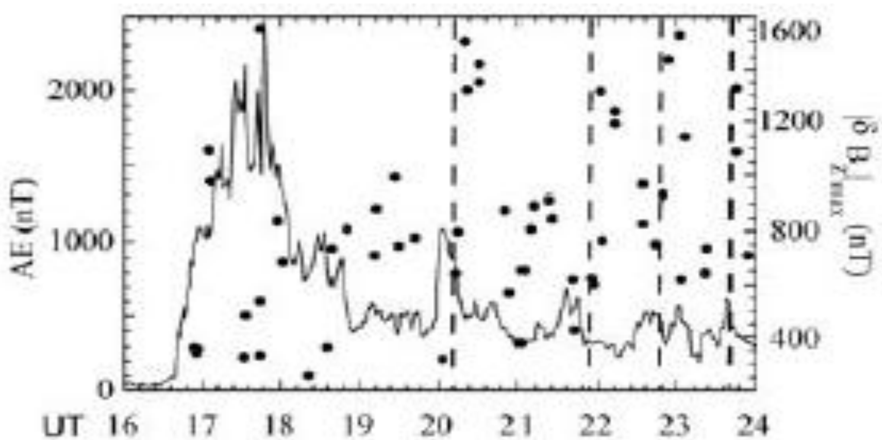

Note the difference in ion/electron spectral characteristics observed by the SSJ4 ESA on DMSP F4 before and after 20:21:15 UT.

It looks as though at 20:21:51UT the electron spectrum became very soft with most of the electron flux below 1 keV. Spectrally this population does not resemble the electron plasma sheet but secondary auroral electrons

This phenomenon repeated four times before minimum Dst with relatively small AE enhancemants

Found in the late main phase of all major storms with Dst min < -200 nT.

Transmission line model

V_{AR} = Alfvén speed in reflection layer

V_{AS} = Alfvén speed at satellite location

$$E_Y = E_{Yi} + E_{Yr} \Rightarrow E_{Yr} = RE_{Yi}$$

$$R = \frac{\Sigma_A - \Sigma_P}{\Sigma_A + \Sigma_P}$$

$$\Sigma_A = 1/\mu_0 V_{AR}$$

$$B_Z = B_{Zi} + B_{Zr}$$

$$\frac{E_{Yi}}{\delta B_{Zi}} = V_{AS} = -\frac{E_{Yr}}{\delta B_{Zr}} = -\frac{RE_{Yi}}{\delta B_{Zr}}$$

$$\delta B_{Zr} = -R\delta B_{Zi}$$

$$\frac{\delta B_Z}{E_Y} = \frac{\delta B_{Zi} + \delta B_{Zr}}{E_{Yi} + E_{Yr}} = \frac{1}{V_{AS}}\frac{1-R}{1+R} = \frac{1}{V_{AS}}\frac{\Sigma_P}{\Sigma_A} = \frac{V_{AR}}{V_{AS}}\mu_0\Sigma_P$$

"Measured" Poynting Flux

$$S_{\|} = \frac{\vec{E}_Y \times \delta\vec{B}_Z}{\mu_0} = \frac{E_Y \delta B_Z}{\mu_0}(1-R^2) = S_{\|i}(1-R^2) = S_{\|i} - S_{\|r}$$

Magnetosphere simulation at 22:00 UT on 6 April 2000

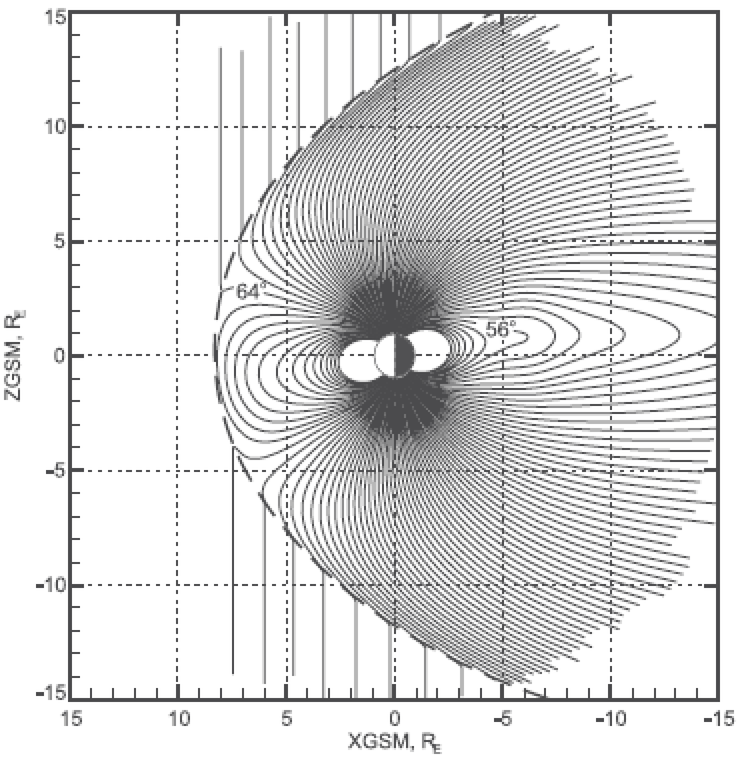

Figure 9. Noon-midnight configuration of the model geomagnetic field lines, corresponding to stormy conditions at UT = 2200 of 6 April 2000. The lines are plotted every 1° in footpoint magnetic latitude, beginning with 50°.

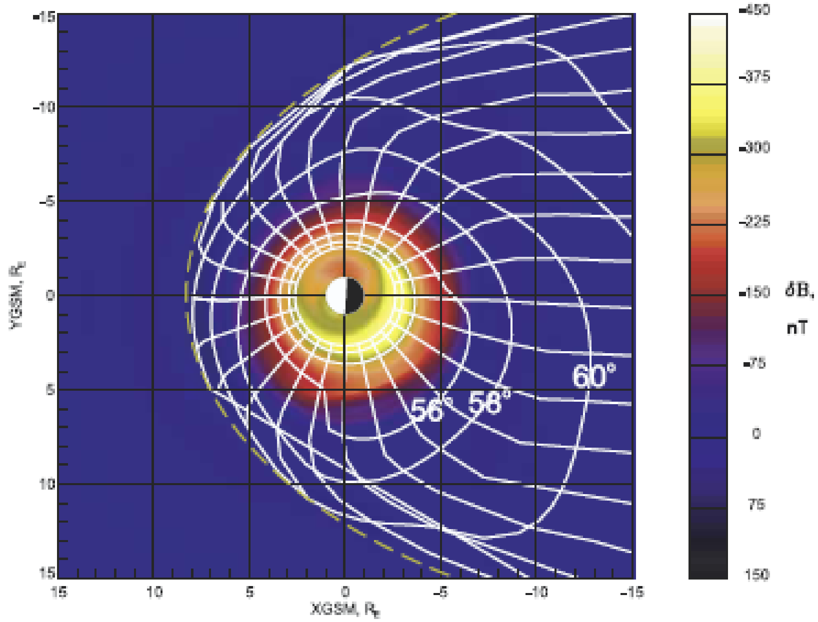

Figure 10. Contours of constant magnetic latitude (at 2° intervals) and constant local time (at 1-hour intervals) at the Earth's surface as mapped along model field lines to the equatorial plane, for the same set of model parameters as in Figure 9, corresponding to UT = 2200 of 6 April 2000. The background color displays the equatorial distribution of the difference δB between the magnitudes of the total model field and the purely dipolar one.

Tsyganenko, N. A., H. J. Singer, and J. C. Kasper, Storm-time distortion of the inner magnetosphere: How severe can it get? ***J. Geophys. Res.*****,** ***108*** **(A5), 1209, 2003.**

Magnetic Storms, Substorms & Generalized Ohm's Law

During the late main phase of the April 2000 magnetic storm multiple DMSP satellites observed large amplitude FACs with $\Delta\delta B$ > 1300 nT).

Associated electric fields on the night side were very weak suggesting relatively large Σ_P > 25 mho when Robinson formula predicted a small fraction of this amount.

We saw a similar effect during the November 2004 storm. Based on strong EUV fluxes from auroral oval Doug Strickland's model predicted electron fluxes and energies that were <10% of what DMSP measured

No commensurate ΔH measured on ground => Fukushima's theorem?

Do precipitating ions play a significant role in creating and maintaining Σ_P [*Galand and Richmond*, JGR, 2001] ?

Does magnetospheric inflation affect the strange particle distributions and intense FACs?

BOSTON COLLEGE ISR

Magnetic Storms, Substorms & Generalized Ohm's Law

Growth phases occur in the intervals between southward turning of IMF B_Z and expansion-phase onset. They are characterized by:

- **Slow decrease in the H component of the Earth's field at auroral latitudes near midnight.**
- **Thinning of the plasma sheet and intensification of tail field strength.**

We consider growth phase electrodynamics observed by the CRRES satellite near geostationary altitude in the midnight sector.

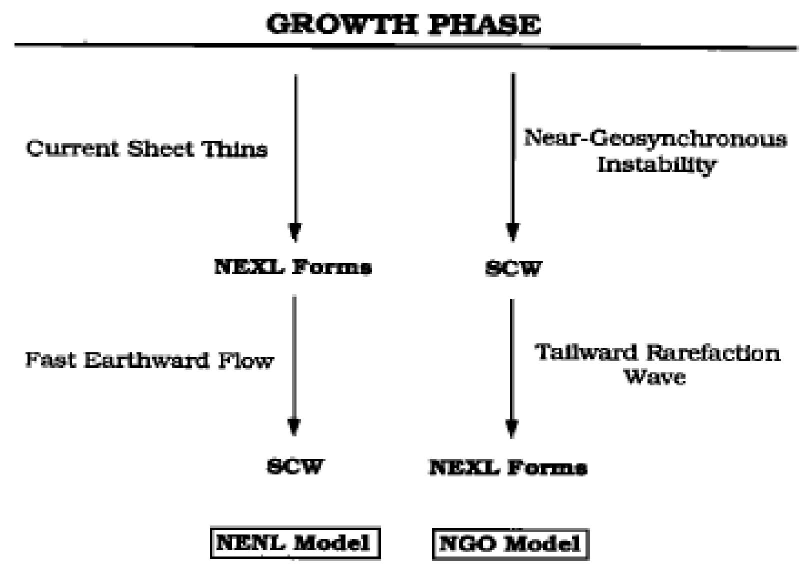

Figure 1. The causal link between near-Earth X line (NEXL) formation and the substorm current wedge (SCW) within the two substorm hypotheses: (left) the near-Earth neutral line (NENL) model and (right) the near-geosynchronous onset (NGO) model.

- McPherron, R. L., Growth phase of magneto-spheric substorms, *JGR, 75*, 5592 – 5599, 1970.

- Lui, A. T. Y., A synthesis of magnetospheric substorm models, *JGR, 96*, 1849, 1991.

- Maynard, et al., Dynamics of the inner magnetosphere near times of substorm onsets, JGR, 101, 7705 - 7736, 1996.

- Erickson et al., Electrodynamics of substorm onsets in the near-geosynchronous plasma sheet, *JGR, 105*, 25,265 – 25,290, 2000.

CRRES measurements near local midnight and geostationary altitude during times of isolates substorm growth and expansion phase onsets

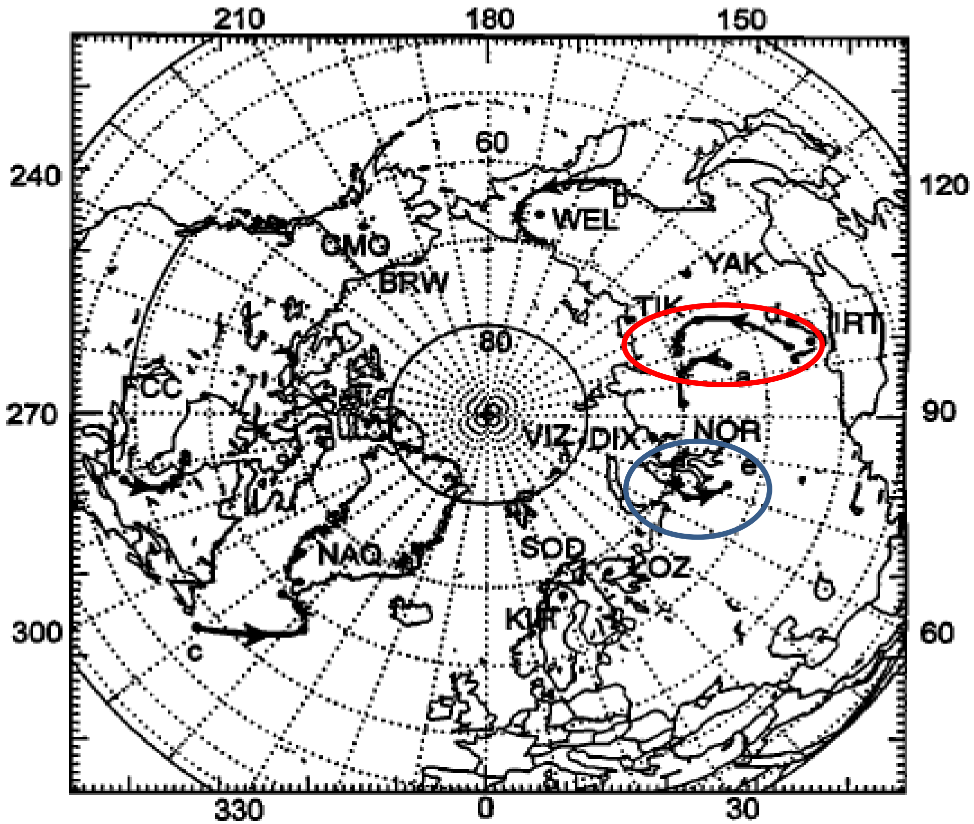

Ionospheric footprints of CRRES trajectories during orbits 535 (red) and 540 (blue).

Magnetic Storms, Substorms & Generalized Ohm's Law

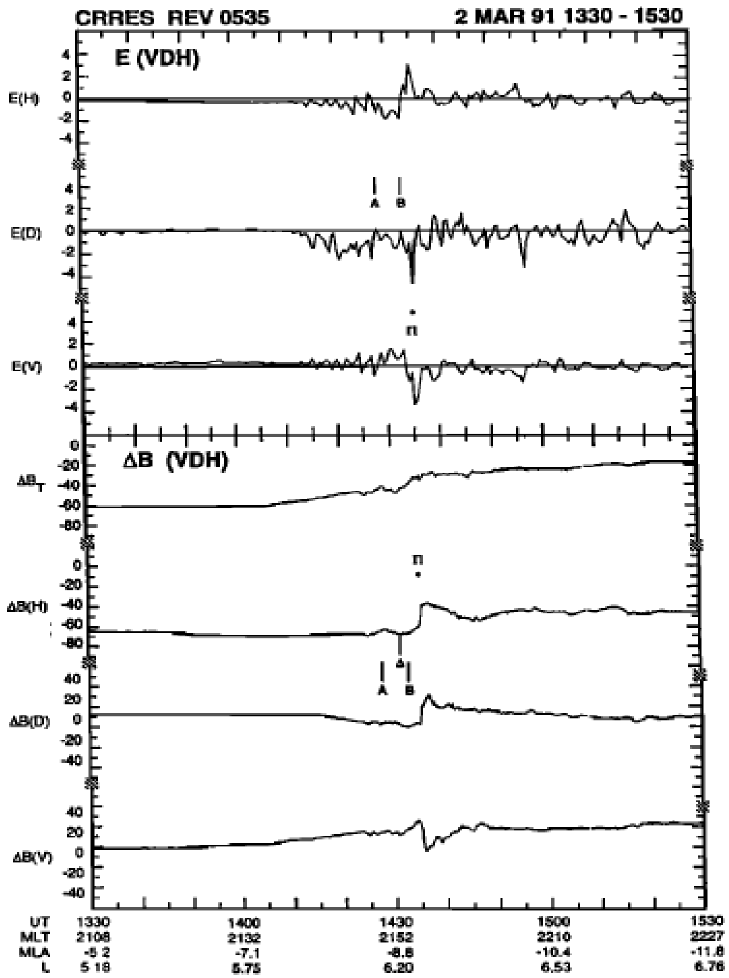

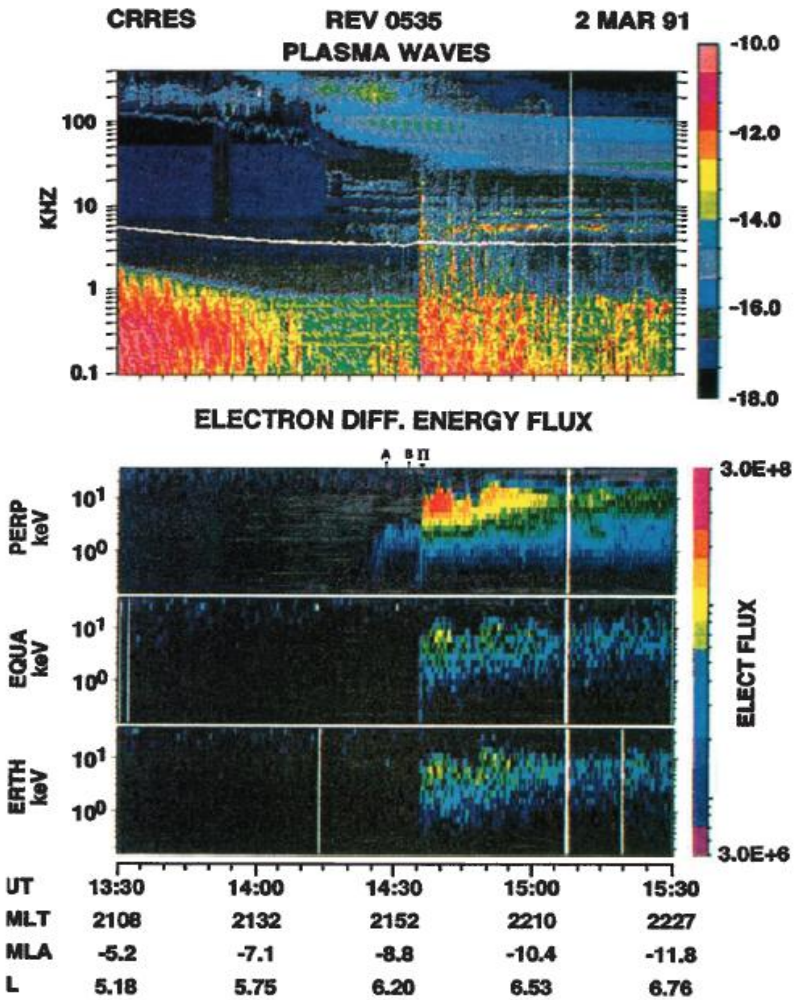

Magnetic Storms, Substorms & Generalized Ohm's Law

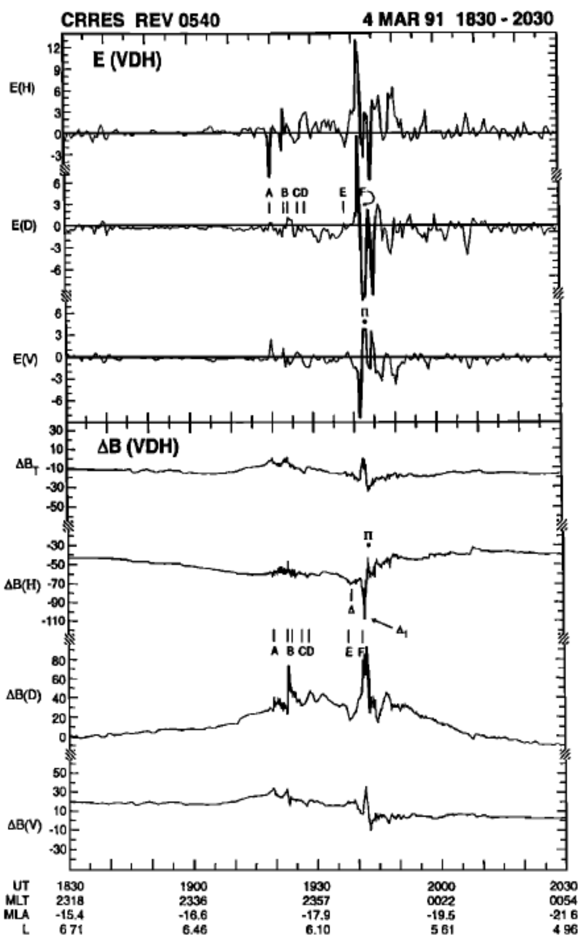

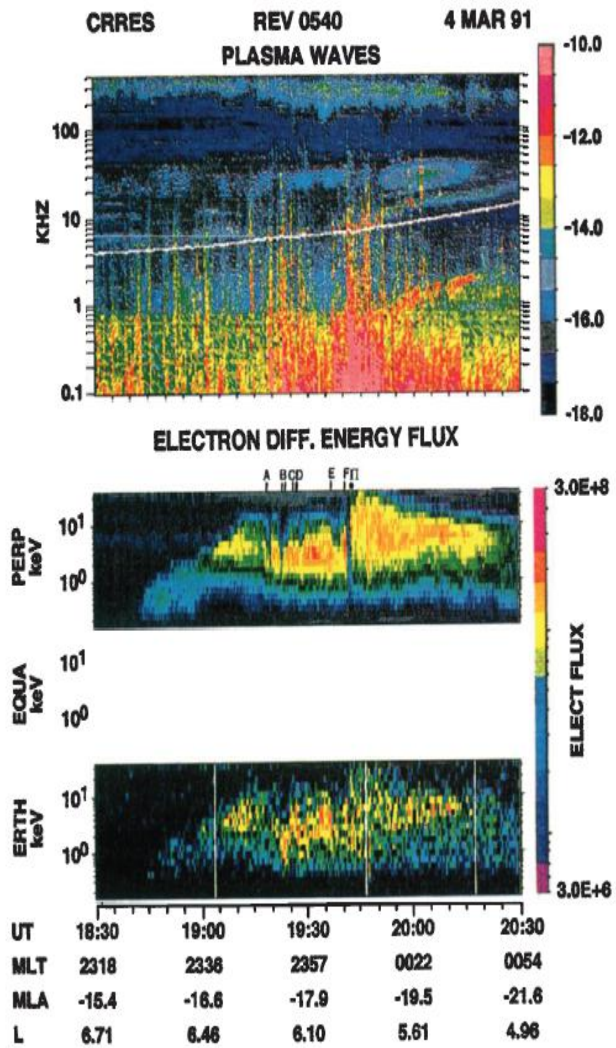

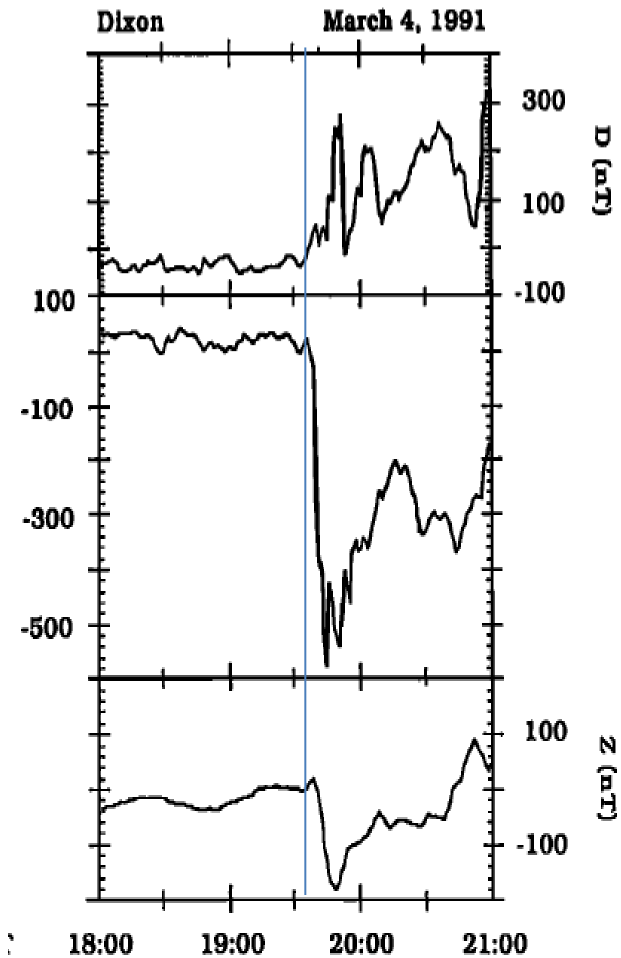

Magnetic Storms, Substorms & Generalized Ohm's Law

Erickson et al., JGR 2000: Studied 20 isolated substorm events observed by CRRES. We will summarize one in which the CRRES orbit (461) mapped to Canadian sector

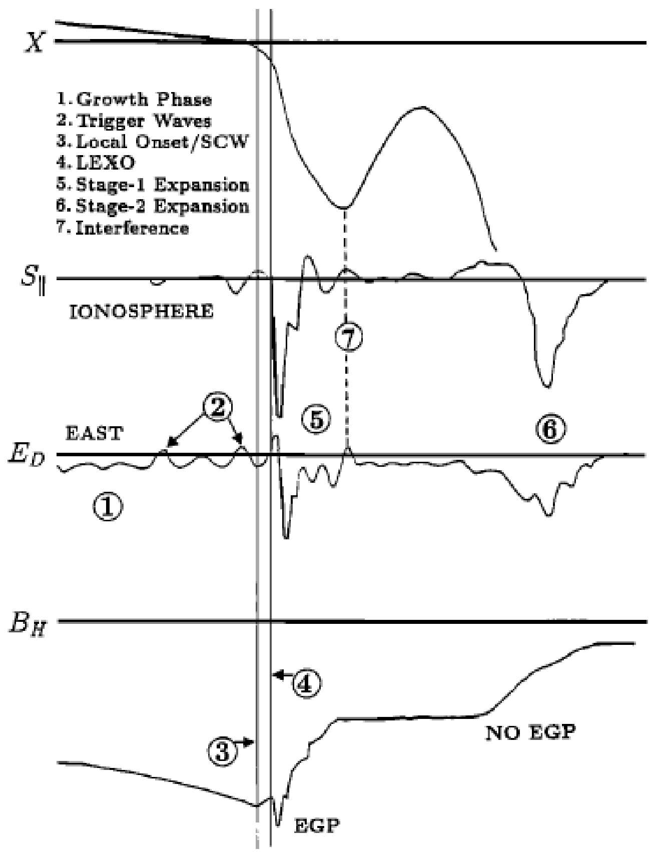

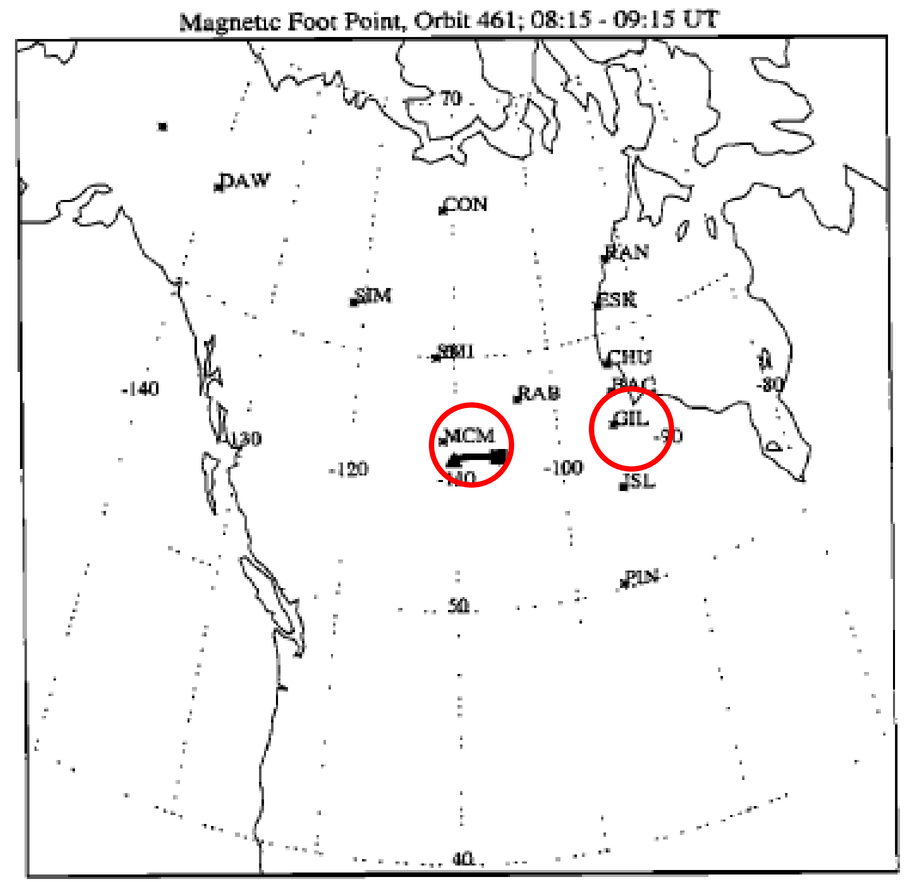

LEXO = local explosive onset
EXP = explosive growth phase

Magnetic Storms, Substorms & Generalized Ohm's Law

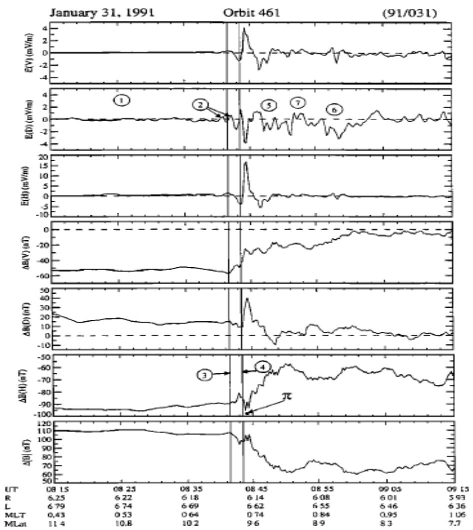

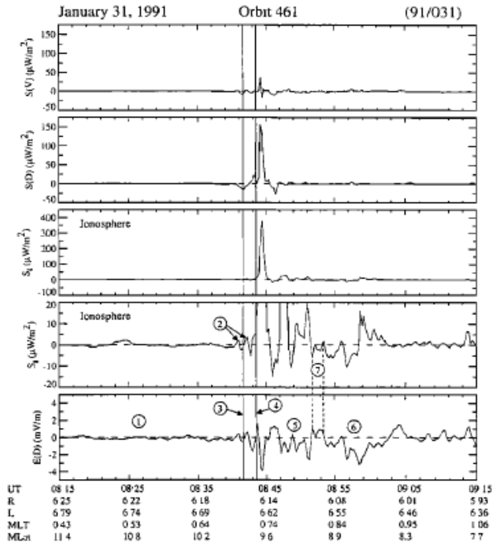

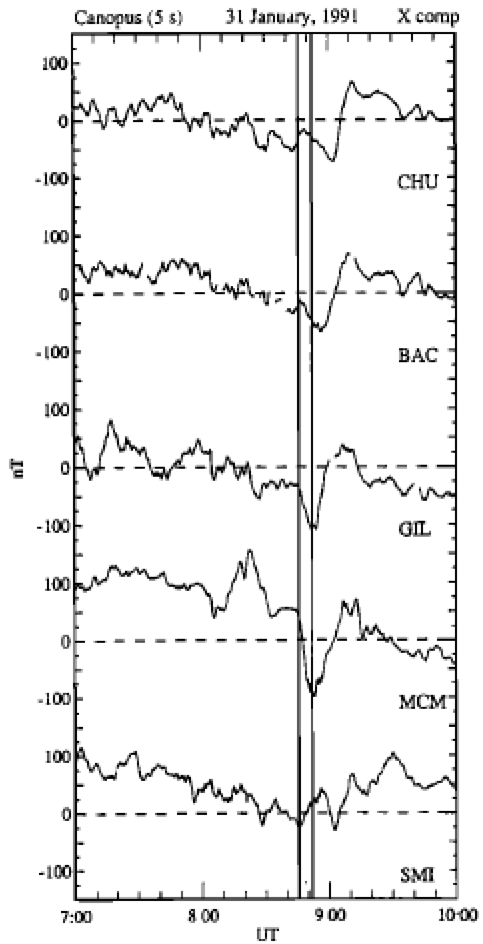

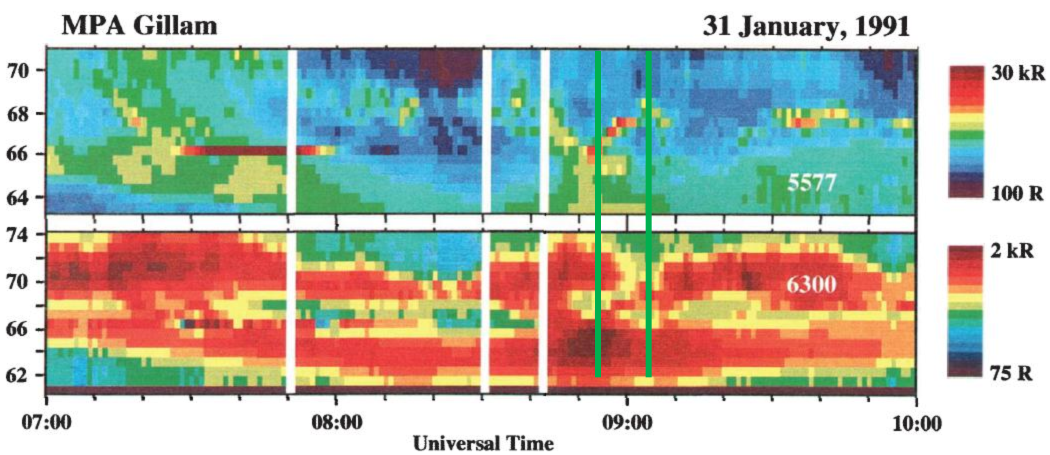

The Bottom Line:

The substorm problem has been with us for a long time. In the 1970s the concepts of near-Earth neutral-line reconnection and disruption of the cross-tail current sheet were widely discussed.

To this day there are pitched battles between which has precedence in substorm onset.

CRRES data seem to support the substorm current wedge model.

During the growth phase the electric field oscillations have little to no associated magnetic perturbations and no measurable field-aligned currents or Poynting flux. (An electrostatic gradient-drift mode that leaves no foot prints on Earth)

This ends when δE becomes large and $E_{total} = E_0 + \delta E$ turns eastward and $j \cdot E_{total} < 0$. Region becomes a local generator coupling the originally electrostatic to an electromagnetic Alfvén model that carries $j_{||}$ and $S_{||}$ to the ionosphere. Pi 2 waves seen when Alfvén waves reach the ionosphere.

Generalized Ohm's Law

Vasyliunas (1975) wrote the generalized Ohm's law in the form

$$\vec{E}+\vec{V}\times\vec{B}=\eta\vec{j}+\frac{m_e}{ne^2}\left[\frac{\partial\vec{j}}{\partial t}+\nabla\cdot(\vec{J}\vec{V}+\vec{V}\vec{J})\right]-\frac{1}{ne}\left[\nabla\cdot\vec{P}_e-\vec{j}\times\vec{B}\right]$$

In ideal MHD the right hand side is zero and **E** = **-** **V** × **B.** With the instrumentation on CLUSTER it is possible to calculate **V** for ions and measure the components of **B** and **E** to identify regions where the MHD approximation breaks down.

Scudder et al 2008 defined a parameter $\delta_{i,\,e}$ that can be used to identify regions where the gyrotropic approximations for ions and/or electrons breakdown :

$$\delta_{i,e}=\frac{\vec{E}_\perp-\vec{V}_{i,e}\times\vec{B}}{w_{\perp i,e}B}$$

The symbol *w* represents the mean thermal speed. If $\delta_{i,\,e}\longrightarrow 1$ indicates that a species is no longer magnetized. Very useful tool near merging lines!

Scudder, J. D., R. D. Holdaway, R. Glassberg, and R. S. Rodriguez (2008), Electron diffusion region and thermal demagnetization, *J. Geophys. Res.*, *113*, A10208, doi:10.1029/2008JA013361.

Vasyliunas, V. M. (1975), Theoretical models of magnetic field line merging, *Rev. Geophys.*, *13*, 303–336, doi:10.1029/RG013i001p00303

CLUSTER Constellation

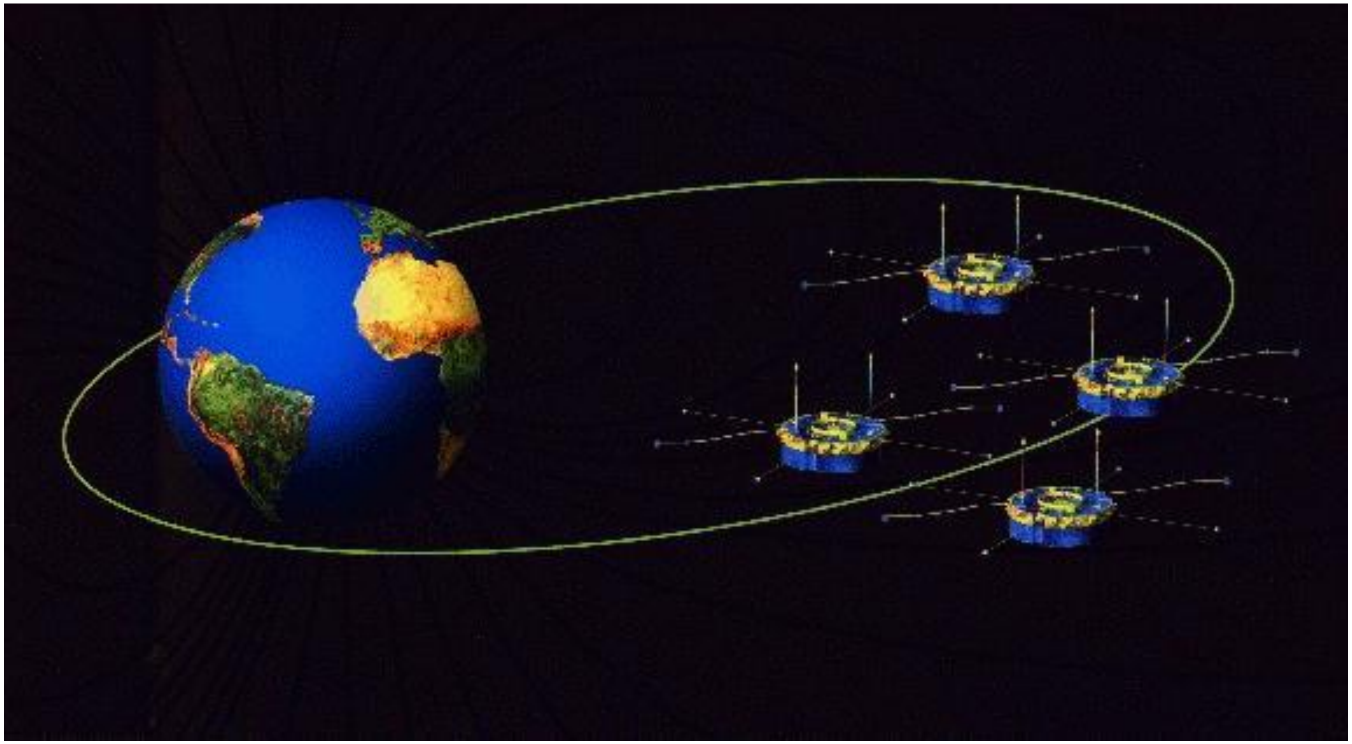

Launch: July/August 2002 into elliptical orbit with 90º inclination
Formation: Variable, tetrahedron most useful for calculating $\nabla \times B$.
Payload includes sensors to measure: particle distribution, electric and magnetic fields as well as wave spectral characteristics.

In a previous lecture we considered Vasyliunas' formula for $j_{\|}$.

$$\nabla p = \vec{j} \times \vec{B} \rightarrow \vec{j} = \frac{\vec{B} \times \nabla p}{B^2}$$

$$\nabla \cdot \vec{j} = 0 \rightarrow \nabla_{\perp} \cdot \vec{j} = -B \frac{\partial (j_{\|} / B)}{\partial s}$$

$$j_{\|} = (B_i / B_e)(\nabla p \times \nabla V)$$

where the symbol V represents the flux tube volume.

Rossi and Olbert (Chapter 9) show that there are three contributors:

(1) The diamagnetic current $\mathbf{j}_D = \nabla \times \mathbf{M}$

$$\vec{j}_D = \frac{\vec{B}}{B^2} \times \nabla P_{\perp} - P_{\perp} \left(\frac{\vec{B}}{B^3} \times \nabla B + \frac{\vec{B}}{B^4} \times [(\vec{B} \cdot \nabla]\vec{B}) \right)$$

(2) The gradient-curvature drift terms j_{GC}

$$\vec{j}_{GC} = P_{\perp} \left(\frac{\vec{B}}{B^2} \times \nabla B \right) + \left(\frac{P_{\|} - P_{\perp}}{B^4} \right) (\vec{B} \times [(\vec{B} \cdot \nabla]\vec{B})$$

The total current $\mathbf{j}_T = \mathbf{j}_D + \mathbf{j}_{GC}$

$$\vec{j}_T = \frac{\vec{B}}{B^2}\times\nabla P_\perp + \left(\frac{P_\parallel - P_\perp}{B^4}\right)(\vec{B}\times[(\vec{B}\cdot\nabla]\vec{B})$$

Thus, $\mathbf{j}_T \times \mathbf{B}$

$$\vec{j}_T \times \vec{B} = \nabla P_\perp + \left(\frac{P_\parallel - P_\perp}{B^2}\right)[(\vec{B}\cdot\nabla]\vec{B}$$

For an isotropic plasma

$$\vec{j}_T \times \vec{B} = \nabla p$$

Since the divergence of the curl of any vector is zero ($\nabla \cdot \mathbf{j}_D) = 0$ only the gradient-curvature currents can contribute to $\mathbf{j}_\parallel$.